

The prelude to the deep minimum between solar cycles 23 and 24: Interplanetary scintillation signatures in the inner heliosphere

P. Janardhan,¹ Susanta Kumar Bisoi,¹ S. Ananthkrishnan,² M. Tokumaru,³ and K. Fujiki³

Received 10 August 2011; revised 28 September 2011; accepted 28 September 2011; published 29 October 2011.

[1] Extensive interplanetary scintillation (IPS) observations at 327 MHz obtained between 1983 and 2009 clearly show a steady and significant drop in the turbulence levels in the entire inner heliosphere starting from around ~1995. We believe that this large-scale IPS signature, in the inner heliosphere, coupled with the fact that solar polar fields have also been declining since ~1995, provide a consistent result showing that the buildup to the deepest minimum in 100 years actually began more than a decade earlier. **Citation:** Janardhan, P., S. K. Bisoi, S. Ananthkrishnan, M. Tokumaru, and K. Fujiki (2011), The prelude to the deep minimum between solar cycles 23 and 24: Interplanetary scintillation signatures in the inner heliosphere, *Geophys. Res. Lett.*, 38, L20108, doi:10.1029/2011GL049227.

1. Introduction

[2] The sunspot minimum at the end of cycle 23, has been one of the deepest we have experienced in the past 100 years with the first spots of the new cycle 24 appearing only in March 2010 instead of December 2008 as was expected. Also, the number of spotless days experienced in 2008 and 2009 was over 70%. Apart from this, Cycle 23 has shown a slower than average field reversal, a slower rise to maximum than other odd numbered cycles, and a second maximum during the declining phase that is unusual for odd-numbered cycles. Though these deviations from “normal” behaviour could be significant in understanding the evolution of magnetic fields on the Sun, they do not yield any direct insights into the onset of the deep minimum experienced at the end of cycle 23. This is because predictions of the strength of solar cycles and the nature of their minima are strongly dictated by both the strength of the ongoing cycle [Dikpati *et al.*, 2006; Choudhuri *et al.*, 2007] and changes in the flow rates of the meridional circulation [Nandy *et al.*, 2011].

[3] Ulysses, the only spacecraft to have explored the mid- and high-latitude heliosphere, in its three solar orbits, provided the earliest indications of the global changes taking place in the solar wind. A significant result from the Ulysses mission came from observations of $|B_r|$, the radial component of the interplanetary magnetic field (IMF), as a function of the heliographic distance r which showed that the product $|B_r|r^2$ is independent of the heliographic latitude [Smith *et al.*, 2003; Lockwood *et al.*, 2009]. This result has far reaching con-

sequences in that it essentially enables one to use *in situ*, single-point observations to quantify the open solar flux entering the heliosphere. The second Ulysses orbit, covering the rising to maximum phase of cycle 23, found the solar wind dynamic pressure (momentum flux) to be significantly lower in the post maximum phase of cycle 23 than during its earlier orbit, spanning the declining phase of cycle 22 [Richardson *et al.*, 2001; McComas *et al.*, 2003]. Finally, the third Ulysses orbit (2004–2008) found a global reduction of open magnetic flux and showed an ~20% reduction in both solar wind mass flux and dynamic pressure in cycle 23 as compared to the earlier two cycles [McComas *et al.*, 2008]. In addition, a study using solar wind measurements between 1995–2009 [Jian *et al.*, 2011] has shown that the solar minimum in 2008–2009 has experienced the slowest solar wind with the weakest solar wind dynamic pressure and magnetic field as compared to the earlier 3 cycles. Figure 1 shows the solar magnetic field in the latitude range 45°–78° computed from ground based magnetograms. The filled dots in Figure 1 represent the actual measurements and the open circles are the yearly means with 1σ error bars. The solid line is a smoothed curve. The vertically oriented dashed parallel lines demarcate cycles 22, and 23, respectively and the shaded gray area indicates the time between the expected minimum in cycle 23 and the time when the first spots in cycle 24 actually began to appear.

[4] The method adopted in computing solar magnetic fields shown in Figure 1 and details of the database used has been described by Janardhan *et al.* [2010]. It is clear from Figure 1 that there has been a continuous decline in the magnetic field starting from around 1995. Since the IMF is basically the result of photospheric magnetic fields being continuously swept out into the heliosphere one would expect to see this reflected in the solar wind and interplanetary medium. Due to the fact that the solar wind undergoes an enormous change in densities ranging from $\sim 10^9 \text{ cm}^{-3}$ at the base of the corona [Mann *et al.*, 2003] to $\sim 10 \text{ cm}^{-3}$ at 1 AU, different techniques are needed to study different regions of the solar wind. However, IPS is the only technique that can probe the entire inner-heliosphere using ground based radio telescopes operating at meter wavelengths.

2. The IPS Methodology

[5] IPS is a scattering phenomenon in which one observes distant extragalactic radio sources to detect random temporal variations of their signal intensity (scintillation) which are caused by the scattering suffered when plane electromagnetic radiation from the radio source passes through the turbulent and refracting solar wind [Hewish *et al.*, 1964; Ananthkrishnan *et al.*, 1980; Asai *et al.*, 1998; Manoharan, 2010a; Tokumaru *et al.*, 2010]. Though IPS measures only small-scale (~150 km sized) fluctuations in density and not

¹Astronomy and Astrophysics Division, Physical Research Laboratory, Ahmedabad, India.

²Electronics Science Department, Pune University, Pune, India.

³Solar-Terrestrial Environment Laboratory, Nagoya University, Toyokawa, Japan.

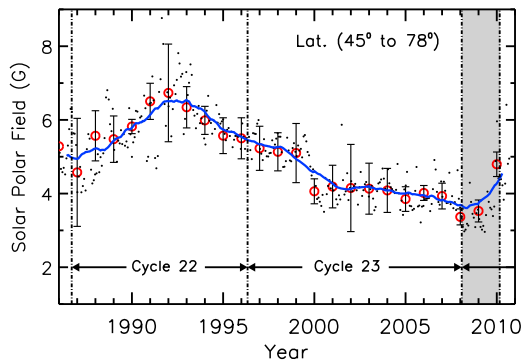


Figure 1. Shows the absolute value of the solar polar field, in the latitude range 45–78°, as a function of time in years for solar cycles 22 and 23.

the bulk density itself, *Hewish et al.* [1985] showed that there was no evidence for enhanced or decreased IPS that was not associated with corresponding variations in density. They went on to derive a relation between a normalized scintillation index denoted ‘g’ and the density given by $g = (Ncm^{-3}/9)^{0.52 \pm 0.05}$. Thus, whenever interplanetary disturbances, containing either enhanced or depleted rms electron density fluctuations (Δn_e) as compared to the background solar wind, cross the line-of-sight (LOS) to the observed source they exhibit themselves as changes in the levels of scintillation (m), i.e., higher or lower than expected m, where $m = \Delta S / \langle S \rangle$ is the ratio of the scintillating flux ΔS to the mean source flux $\langle S \rangle$. In other words, whenever turbulence levels change in the solar wind, they will be reflected in IPS measurements as changes in m. The main advantage of the IPS technique is that, it can probe a very large region of the inner heliosphere, ranging from about 0.2 AU to 0.8 AU and it is extremely sensitive to small changes in Δn_e . In fact IPS is so sensitive to changes in Δn_e that it has been used to probe Δn_e fluctuations in tenuous cometary ion tails well downstream of the nucleus [*Janardhan et al.*, 1992] and to study solar wind disappearance events wherein average densities at 1 AU drop to values below 0.1 cm^{-3} [*Janardhan et al.*, 2005]. In a typical IPS observation, the angle between the Sun the Earth and the observed radio source is known as the solar elongation (ϵ). Please refer to Figure 1 of *Balasubramanian et al.* [2003] for details of the IPS observing geometry. Since the solar wind density beyond ~ 0.2 AU is inversely proportional to r^2 [*Bird et al.*, 1994] where, $r = \sin(\epsilon)$, measurements of m in the direction of a given radio source will increase with decreasing ϵ or distance ‘r’ from the Sun, until a certain ϵ . After this point m falls off sharply with further reduction in ϵ . The ϵ at which m turns over is dependent on frequency and at 327 MHz it lies between 10° and 14° . The region at ϵ larger than the turnover defines the region of weak scattering where the approximation of scattering by a thin screen is valid [*Salpeter*, 1967]. For an ideal point source, m will be unity at an ϵ of $\sim 12^\circ$ and drop to values below unity with increasing distance r. For sources, with finite compact component sizes (>0 milli arcsec (mas)), m will be $<$ unity at the turnover.

[6] For the steady state solar wind, values of m can be computed by obtaining theoretical temporal power spectra using a solar wind model assuming weak scattering and a

power law distribution of density irregularities in the IP medium for any given source size and distance r of the LOS from the Sun [*Marians*, 1975]. The set of six curves (labeled ‘A’) in Figure 2 show the theoretically expected m as a function of ϵ for various source sizes in mas, assuming weak scattering at 327 MHz. To remove the ϵ or distance dependence of m, each observation of m has to be normalized by that of a point source at the corresponding ϵ . It has been shown that the source 1148-001 is ≤ 10 mas in angular extent at 327 MHz. Thus, 1148-001 can be treated as a nearly ideal point source, with most of its flux contained in a scintillating compact component [*Venugopal et al.*, 1985]. Normalizing all observations of m in this manner will yield an ϵ or distance independent value of m as shown for three source sizes (labeled ‘B’) in Figure 2. It must be noted that the curves in Figure 2 imply that the radial fall off rate is slightly different for different source sizes. Thus, the m for the larger source sizes will be over-corrected at large distances. However, most of the observed IPS sources are strong scintillators with sizes ≤ 250 mas and will not suffer from this normalization.

3. The Observations and Data Reduction

[7] The three-station IPS facility, operated by the Solar-Terrestrial Environment Laboratory (STEL), Japan, and used for the observations described in this paper, can carry out IPS observations at 327 MHz on about 200 compact extragalactic, radio sources on a regular basis, to derive solar wind velocities and m. In 1994, a fourth antenna was added to the system to form a four-station network that could provide more robust estimates of the solar wind speed owing to the redundancy in the baseline geometry obtained by having an additional station. We have taken data from 1983 to 2009, which had a one year data gap in 1994 owing to the development of the fourth IPS station, and have chosen sources which had at least 400 individual observations over this period of 27 years. We also ensured that there were no significant data gaps in any given year, apart from the one year gap in 1994. Of the total of 215 sources observed, we were finally left with 26 sources covering the entire 24 hour range of source right ascensions and a wide range of source

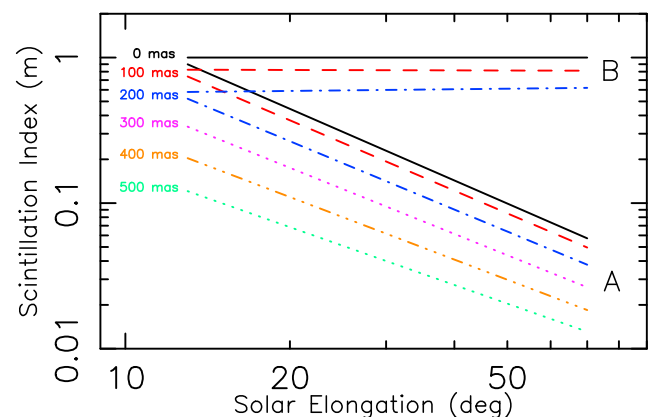


Figure 2. Curves (labeled ‘A’) of theoretically expected m as a function of ϵ for various source sizes. Curves (labeled ‘B’) corresponding to source sizes of 0 mas, 100 mas, and 200 mas, have been normalized by the point source m at the corresponding ϵ .

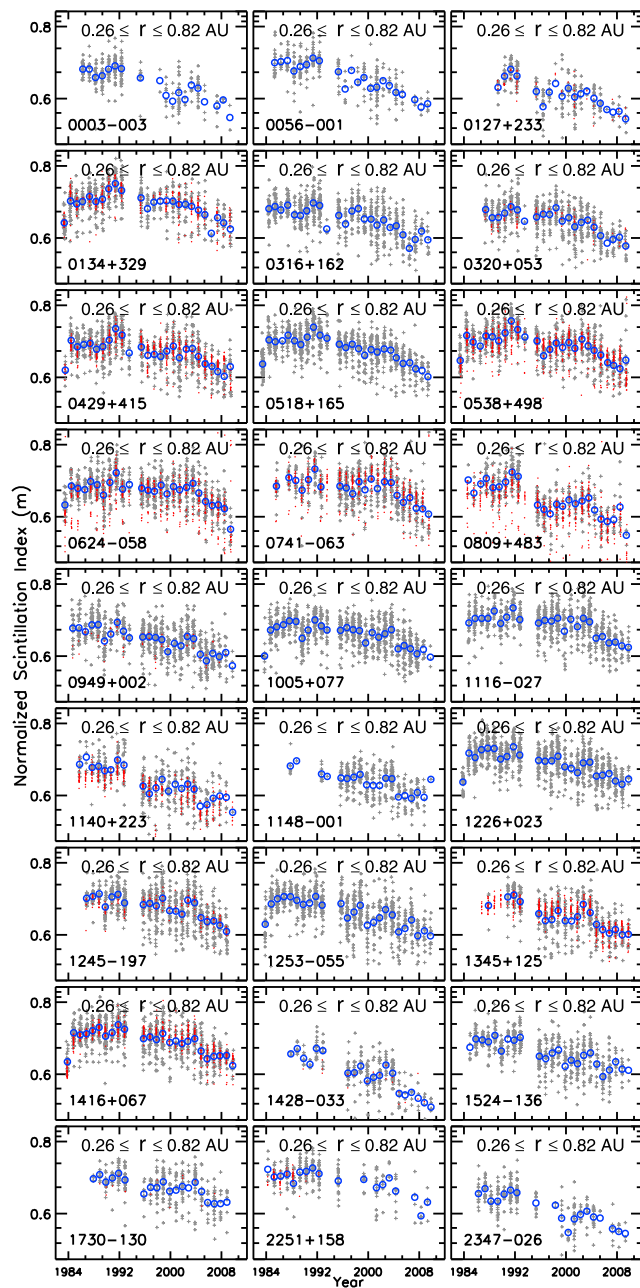


Figure 3. Plots m as a function of time in years for 27 sources after m has been made independent of distance from the Sun by normalizing each observation by the value of m for the source 1148-001. The grey crosses are observations at source helio latitudes $\leq 45^\circ$ while the fine red dots are observations at source heliolatitudes $> 45^\circ$. The open circles are yearly averages by excluding the high latitude observations. The IAU name of each source is indicated at the bottom left in each panel.

declinations. The source 1148-001 was included as the 27th source even though it had some data gaps and therefore did not fully comply with our selection criteria. The data set was first normalized by the highest value so that the range of m was between 0 and unity. The distance dependence of m was then removed by normalizing every individual observation for each source by the value of m for the source 1148-001 at the corresponding ϵ . Figure 3 shows plots of m

as a function of time in years for the 27 chosen sources lying in the distance range 0.26 to 0.82 AU. The grey crosses are measurements when the source heliolatitude is $\leq 45^\circ$ while the fine red dots are measurements when the source heliolatitude is $> 45^\circ$. The large, blue, open circles are yearly averages taken without the high latitude observations. The reason for dropping the high latitude observations from the yearly averages is because IPS observations have shown [Tokumaru *et al.*, 2000] that the solar wind structure changes with the solar cycle, being more or less symmetric at solar maximum and considerably asymmetric during solar minimum. This asymmetry could change the way m falls off with radial distance. Since our IPS measurements mix measurements distant from the Sun near the solar equator with measurements at small ϵ at high solar latitude, we drop the high latitude observations from the yearly averages in order not to affect the yearly means. In addition, long term and gradual changes in the antenna sensitivity caused by degradation in the efficiency of the system, could cause some changes in the IPS measurements over time. Such changes are very difficult to quantify but every effort has been made to maintain the system stability and we believe that these changes cannot account for or explain the systematic drop in m starting from around 1995. It can be seen from Figure 3 that all the sources show a steady decline in m starting from around ~ 1995 implying a reduction in solar wind turbulence levels. The drop in m ranges between 10% and 25% when the annual means are taken considering all observations and it ranges between 10% and 22% when the annual means are taken without including the high latitude observations. The average drop is therefore around 16%. One must note however that only 16 of the 27 sources go to latitudes above 45° while the remaining 11 sources have all observations at heliolatitudes $\leq 45^\circ$. In order to achieve greater clarity and to avoid any confusion caused by showing a large number of panels in Figure 3 the yearly means of each source (blue open circles) are shown again, in Figure 4, as a composite plot of m as a function of time in years. The steady drop in m from ~ 1995 can be unambiguously seen in Figure 4.

4. Discussion and Conclusions

[8] We have seen that the turbulence levels, as indicated by reduced scintillation levels in the IP medium, have dropped steadily since ~ 1995 . In addition, $|B_r|$ has been lower during the recent minima than in the past three

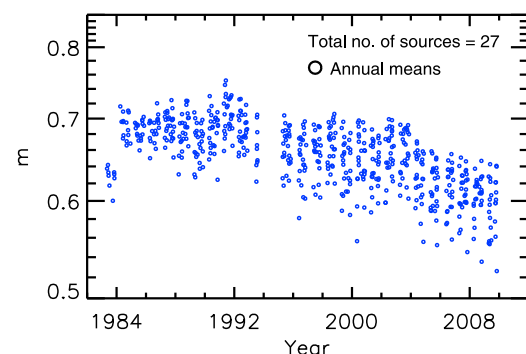


Figure 4. Shows the annual means of m as a function of time for each of the 27 sources shown in Figure 3.

minima [Smith and Balogh, 2008] and solar polar fields have also shown a steep decline since ~1995. Since solar polar fields supply most of the heliospheric magnetic flux during solar minimum conditions [Svalgaard et al., 2005], weaker polar fields imply that the IMF will also be significantly lower. A causal relationship between stronger magnetic fields and turbulence in this region also implies a decrease in turbulence levels over the solar poles since ~1995. It has been shown that the solar wind turbulence is related to both the rms electron density fluctuations (Δn_e) and large scale magnetic field fluctuations in fast solar wind streams [Ananthakrishnan et al., 1980]. Similarly, it is possible that a global reduction in the IMF is being reflected as a large scale global reduction in m (or microturbulence) as shown by our observations. As opposed to our method, IPS observations of the change in the turnover distance of m , which defines the minimum distance (from the sun) at which the weak scattering regime starts, have shown a steady decrease in the scattering diameter of the corona since 2003 [Manoharan, 2010b].

[9] A great deal of work has been done in modeling the solar dynamo and predicting the strength of future solar cycles. It has been argued [Dikpati et al., 2006] that since the meridional circulation period is between 17–21 years in length, the strength of the polar fields during the ongoing cycle minimum and the preceding two solar minima will influence the strength of the next cycle. Another view point is that of Choudhuri et al. [2007] who claim that only the value of the polar field strength in the ongoing cycle minimum is important in predicting the next cycle. Very recently, Nandy et al. [2011] used a kinematic dynamo simulation model that adjusted the flow speeds in each half of the cycle to reproduce the extended minimum in cycle 23. Their model showed that the changes in the meridional flow speeds that led to the extended minimum began as early as the mid to late 1990's and also predicted that very deep minima are generally associated with weak polar fields. On the other hand, using observations, from cycles 21, 22 and 23, of the drift of Fe XIV emission features over time at high latitudes, referred to as “rush to the poles” Alrock [2011] was able to show that the solar maximum occurs approximately 1.5 years prior to the rush-to-the-poles reaching the solar poles.

[10] In conclusion, our observations have shown that turbulence levels in the inner heliosphere have shown a steady decline since the mid 90's. The fact that the change in the meridional flow that regulates the solar dynamo began in the mid 1990's coupled with the fact that solar polar fields have been declining since ~1995 and our IPS observations all provide a consistent result showing that the buildup to the deepest minimum in 100 years actually began more than a decade earlier.

[11] **Acknowledgments.** IPS observations were carried out under the solar wind program of STEL, Japan. We thank the two anonymous referees whose comments have improved the paper significantly. One of the authors (JP) thanks Bill Coles, Mike Bird and Murray Dryer for their critical comments.

[12] The Editor thanks two anonymous reviewers for their assistance in evaluating this paper.

References

- Alrock, R. C. (2011), Coronal Fe XIV emission during the whole heliosphere interval campaign, *Sol. Phys.*, doi:10.1007/s11207-011-9714-9, in press.
- Ananthakrishnan, S., W. A. Coles, and J. J. Kaufman (1980), Microturbulence in solar wind streams, *J. Geophys. Res.*, *85*, 6025–6030.
- Asai, K., M. Kojima, M. Tokumaru, A. Yokobe, B. V. Jackson, P. L. Hick, and P. K. Manoharan (1998), Heliospheric tomography using interplanetary scintillation observations: 3. Correlation between speed and electron density fluctuations in the solar wind, *J. Geophys. Res.*, *103*, 1991–2001.
- Balasubramanian, V., P. Janardhan, S. Srinivasan, and S. Ananthakrishnan (2003), Interplanetary scintillation observations of the solar wind disappearance event of May 1999, *J. Geophys. Res.*, *108*(A3), 1121, doi:10.1029/2002JA009516.
- Bird, M. K., H. Volland, M. Paetzold, P. Edenhofer, S. W. Asmar, and J. P. Brenkle (1994), The coronal electron density distribution determined from dual-frequency ranging measurements during the 1991 solar conjunction of the ULYSSES spacecraft, *Astrophys. J.*, *426*, 373–381.
- Choudhuri, A. R., P. Chatterjee, and J. Jiang (2007), Predicting solar cycle 24 with a solar dynamo model, *Phys. Rev. Lett.*, *98*(13), 131103, doi:10.1103/PhysRevLett.98.131103.
- Dikpati, M., G. de Toma, and P. A. Gilman (2006), Predicting the strength of solar cycle 24 using a flux-transport dynamo-based tool, *Geophys. Res. Lett.*, *33*, L05102, doi:10.1029/2005GL025221.
- Hewish, A., P. F. Scott, and D. Wills (1964), Interplanetary scintillation of small diameter radio sources, *Nature*, *203*, 1214–1217.
- Hewish, A., S. J. Tappin, and G. R. Gapper (1985), Origin of strong interplanetary shocks, *Nature*, *314*, 137–140.
- Janardhan, P., S. K. Alurkar, A. D. Bobra, O. B. Slee, and D. Waldron (1992), Power spectral analysis of enhanced scintillation of quasar 3C459 due to Comet Halley, *Aust. J. Phys.*, *45*, 115–126.
- Janardhan, P., K. Fujiki, M. Kojima, M. Tokumaru, and K. Hakamada (2005), Resolving the enigmatic solar wind disappearance event of 11 May 1999, *J. Geophys. Res.*, *110*, A08101, doi:10.1029/2004JA010535.
- Janardhan, P., S. K. Bisoi, and S. Gosain (2010), Solar polar fields during cycles 21–23: Correlation with meridional flows, *Sol. Phys.*, *267*, 267–277.
- Jian, L. K., C. T. Russell, and J. G. Luhmann (2011), Comparing solar minimum 23/24 with historical solar wind records at 1 AU, *Sol. Phys.*, doi:10.1007/s11207-011-9737-2, in press.
- Lockwood, M., M. Owens, and A. P. Rouillard (2009), Excess open solar magnetic flux from satellite data: 1. Analysis of the third perihelion Ulysses pass, *J. Geophys. Res.*, *114*, A11103, doi:10.1029/2009JA014449.
- Mann, G., A. Klassen, H. Aurass, and H. Classen (2003), Formation and development of shock waves in the solar corona and the near-Sun interplanetary space, *Astron. Astrophys.*, *400*, 329–336.
- Manoharan, P. K. (2010a), Ooty interplanetary scintillation—Remote-sensing observations and analysis of coronal mass ejections in the heliosphere, *Sol. Phys.*, *265*, 137–157.
- Manoharan, P. K. (2010b), Peculiar current solar-minimum structure of the heliosphere, *Highlights Astron.*, *15*, 484–487.
- Marians, M. (1975), Computed scintillation spectra for strong turbulence, *Radio Sci.*, *10*, 115–119.
- McComas, D. J., H. A. Elliott, N. A. Schwadron, J. T. Gosling, R. M. Skoug, and B. E. Goldstein (2003), The three-dimensional solar wind around solar maximum, *Geophys. Res. Lett.*, *30*(10), 1517, doi:10.1029/2003GL017136.
- McComas, D. J., R. W. Ebert, H. A. Elliott, B. E. Goldstein, J. T. Gosling, N. A. Schwadron, and R. M. Skoug (2008), Weaker solar wind from the polar coronal holes and the whole Sun, *Geophys. Res. Lett.*, *35*, L18103, doi:10.1029/2008GL034896.
- Nandy, D., A. Muñoz-Jaramillo, and P. C. H. Martens (2011), The unusual minimum of sunspot cycle 23 caused by meridional plasma flow variations, *Nature*, *471*, 80–82.
- Richardson, J. D., C. Wang, and K. I. Paularena (2001), The solar wind: From solar minimum to solar maximum, *Adv. Space Res.*, *27*, 471–479.
- Salpeter, E. E. (1967), Interplanetary scintillations. I. Theory, *Astrophys. J.*, *147*, 433.
- Smith, E. J., and A. Balogh (2008), Decrease in heliospheric magnetic flux in this solar minimum: Recent Ulysses magnetic field observations, *Geophys. Res. Lett.*, *35*, L22103, doi:10.1029/2008GL035345.
- Smith, E. J., et al. (2003), The Sun and heliosphere at solar maximum, *Science*, *302*, 1165–1169.
- Svalgaard, L., E. W. Cliver, and Y. Kamide (2005), Sunspot cycle 24: Smallest cycle in 100 years?, *Geophys. Res. Lett.*, *32*, L01104, doi:10.1029/2004GL021664.
- Tokumaru, M., M. Kojima, Y. Ishida, A. Yokobe, and T. Ohmi (2000), Large-scale structure of solar wind turbulence near solar activity minimum, *Adv. Space Res.*, *25*, 1943–1946.
- Tokumaru, M., M. Kojima, and K. Fujiki (2010), Solar cycle evolution of the solar wind speed distribution from 1985 to 2008, *J. Geophys. Res.*, *115*, A04102, doi:10.1029/2009JA014628.

Venugopal, V. R., S. Ananthkrishnan, G. Swarup, A. V. Pynzar, and V. A. Udaltsov (1985), Structure of PKS 1148-001, *Mon. Not. R. Astron. Soc.*, 215, 685–689.

S. Ananthkrishnan, Electronics Science Department, Pune University, Pune, Maharashtra 411 007, India. (subra.anan@gmail.com)

K. Fujiki and M. Tokumaru, Solar-Terrestrial Environment Laboratory, Nagoya University, Honohara 3-13, Toyokawa, Aichi 442-8507, Japan. (fujiki@stelab.nagoya-u.ac.jp; tokumaru@stelab.nagoya-u.ac.jp)

P. Janardhan and S. K. Bisoi, Astronomy and Astrophysics Division, Physical Research Laboratory, Ahmedabad, Gujarat 380 009, India. (jerry@prl.res.in; susanta@prl.res.in)